Chapter 9

Protein Aggregation

9.1 Proteins and Colloids

In all biotechnological applications which involve proteins, particular attention must be given to the stability of the complex protein structure to guarantee proper function. Indeed, proteins are exposed to a broad range of chemical and physical instabilities, which can modify their structure and deteriorate their activity.

• Chemical instabilities include oxydation, deamidation, asparic acid isomerization, peptide fragmentation, nonreducible cross-linking.

• Physical instabilities are represented mainly by protein aggregation. Aggregation of therapeutic proteins is a significant hurdle in protein drug development, hindering rapid commercialization of potential drug candidates. Aggregation is indeed the major protein instability encountered in almost all stages of therapeutic protein manufacturing, including expression from the cells, purification, storage, shipping and administration to the patient. About $20 - 25\%$ of the approved therapeutic proteins are administred subcutaneously via injections and are formulated as solutions at high protein concentrations (50-200 mg/mL) in order to reduce the injection volumes below 1.5-2 mL. Such high concentrations can clearly promote interactions and aggregation. Since the presence of protein aggregates in pharmaceuticals may compromise drug safety and drug efficacy, the protein aggregate content must be strictly controlled to assure satisfactory product quality. There is therefore a severe need to increase our understanding of the mechanisms of protein aggregation at a fundamental level with the aim of optimizing the protein primary sequence and/or the operative parameters, e.g. the solution composition in terms of pH, type and concentration of excipients.

This challenge is again a colloidal stability problem. Protein sizes are indeed typically in

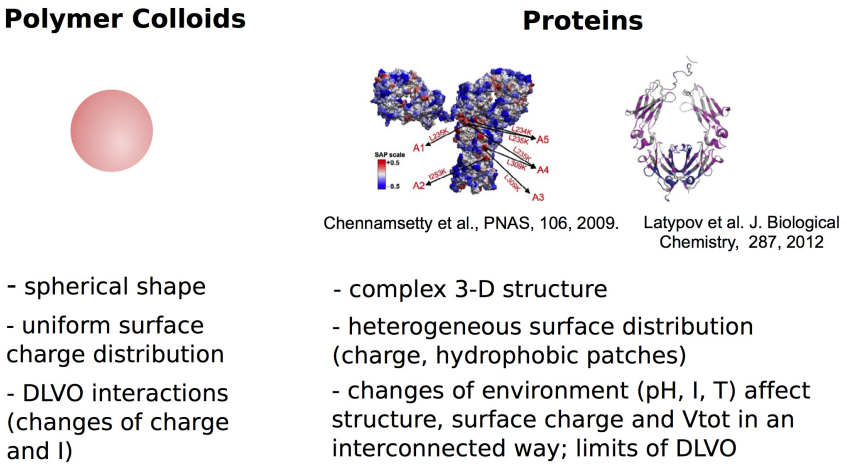

Figure 9.1: Key differences between proteins and polymer colloids

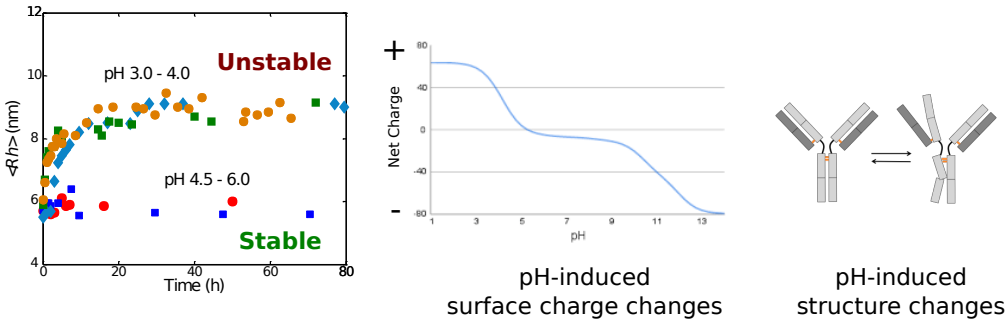

Figure 9.2: Example of the aggregation behavior of a monoclonal antibody solution at low pH

the order of a few nanometers, and are thus lying in the colloidal range. Proteins are therefore small enough to be affected by Brownian motion, but sufficiently large compared to solvent molecules so that the solvent can be considered as a continuum. Several of the concepts and techniques discussed in Chapters 1-7 for polymers apply also to proteins, in particular for globular aggregates formed by folded proteins. For instance, several protein aggregates exhibit fractal morphology, in analogy with polymer clusters. Light scattering techniques are often used to characterize the structure of protein gels in terms of fractal dimension. However, there are crucial differences between proteins and polymer colloids, mainly because of the complex protein secondary and tertiary structure.

To explain this difference, we use as an example the stability of a monoclonal antibody at low pH: the aggregation stability, which is followed by monitoring the increase during time of the average radius of the population, decreases with increases pH value (Figure 9.2). From a colloidal point of view, the net charge of a protein increases with the increase of the difference between the pH and the pI value. However, the low pH values modify the secondary and tertiary structures of the proteins; following these unfolding events, reactive hydrophobic patches can be exposed to the exterior, and the attractive hydrophobic forces can overcome the electrostatic repulsive interactions. This example explains clearly how for proteins there is the need to characterize simultaneously aggregation and structural stability. As a consequence of this complexity, the DLVO theory has only limited applications.

9.2 Experimental biophysical techniques

In protein science, and in particular in problems dealing with protein aggregation and self-assembly, experimental analytics is a fundamental aspect and represents the first step to perform any mechanistic study. Protein systems typically exhibit a series of challenges including very low and high values of proteins concentrations, presence of dynamic equilibria and very heterogeneous mixtures, with presence of species ranging from few nm to several microns.

As discussed before, with respect to colloidal systems, there is the need to characterize not only the size and shape of the aggregates but also potential changes in the structure of the protein species. In addition, more practical limitations of laboratory experiments related to the small volumes and amounts of material which are normally available have also to be considered. Currently, there is not a single technique capable of providing all the required information. Rather, a bactery of different approaches has to be applied in parallel (Figure 9.3).

Size and Molecular Weight: In analogy with colloidal systems, light scattering (Chapter 7) represents one of the most important techniques to achieve information about the size and the shape of the protein aggregates which are generated during the aggregation reaction. Static Light Scattering (SLS) and Dynamic Light Scattering (DLS) can be used to follow the increase in the average gyration radius ($< R_g >$) and in the average hydrodynamic radius ($< R_h >$), respectively, as well to measure the fractal dimension of the aggregates.

However, light scattering is challenging to apply for the analysis of the heterogeneous mixtures typically observed during the aggregation of proteins in solution. In particular, from the average signal recorded in bulk experiments is difficult to de-convolute information about the

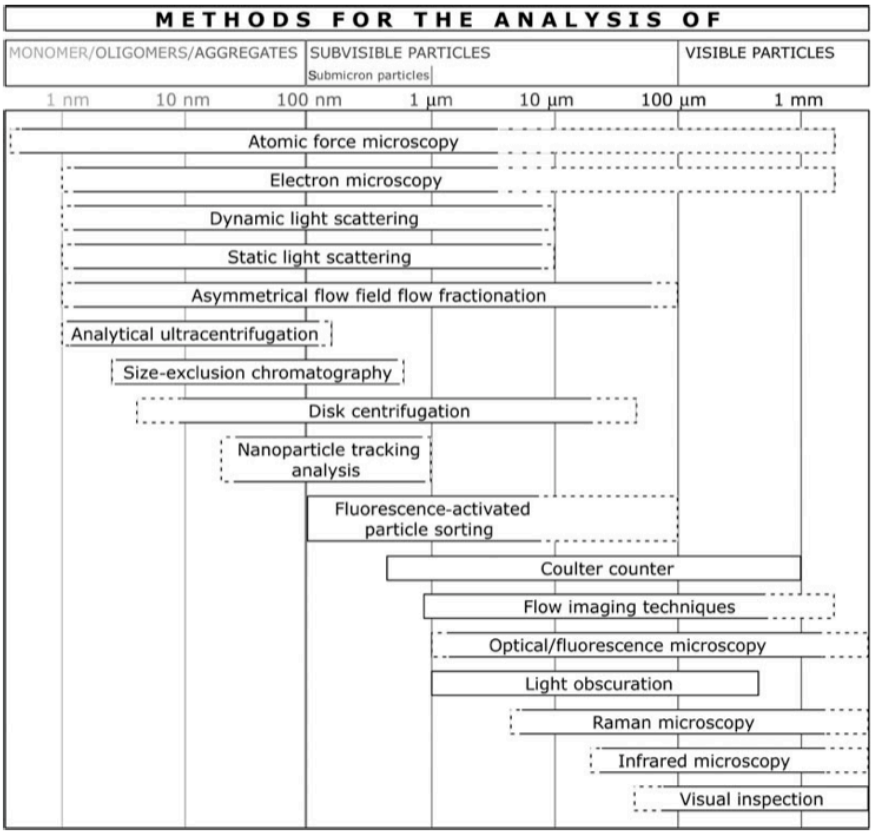

Figure 9.3: Overview of conventional biophysical methods to investigate protein aggregates over different length scale. Zoells S. et al., J. Pharm, Sci, 101,3, 914-935 2012

full size distribution.

An attractive strategy to address this limitation consists in performing the fractionation of the protein mixtures before analyzing individually the fractionated species. The most common method is represented by **Size Exclusion Chromatography coupled with inline multi angle light scattering**. Limit of the size of the aggregates that can be detected, used to quantify the residual monomer and the oligomer distribution (see Figure 9.4 (a)).

Secondary and Tertiary Structure: In order to characterize the structure of the protein, circular dichroism and Fourier Transform Infrared Spectroscopy are some of the most common methods.

Protein stability: Isothermal Calorimetry and differential scanning calorimetry.

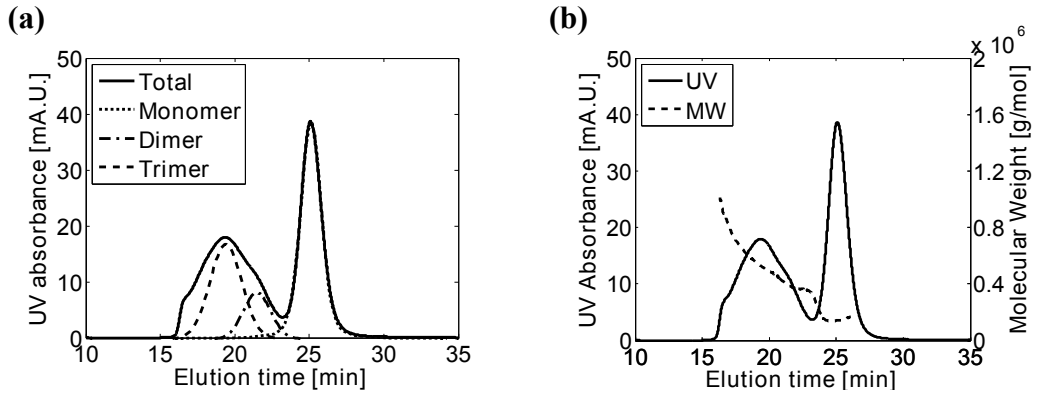

Figure 9.4: Typical SEC chromatogram of a mixture of mAb monomer and mAb aggregates. (a) Determination of the monomer, dimer and trimer content by peak deconvolution (b) Measure of the aggregate molecular weight from Multi Angle Light Scattering.

Microfluidics Very recently, microfluidics is emerging a very powerful tool to address many of the limitations of conventional biophysical methods. Attractive advantages include not only small volumes and short analysis times, but also the possibility to couple different strategies on the same platform, the more accurate control of mass and heat transport and the ability to compartmentalize solutions in droplets.

9.3 Kinetic Model and PBE

Many possible aggregation mechanisms have been observed. With respect to colloid systems, also structure changes and nucleation events must be considered in addition to growth, which can occur either via monomer addition or cluster-cluster aggregation. In many applications it is importat to discover which mechanism is the one in action.

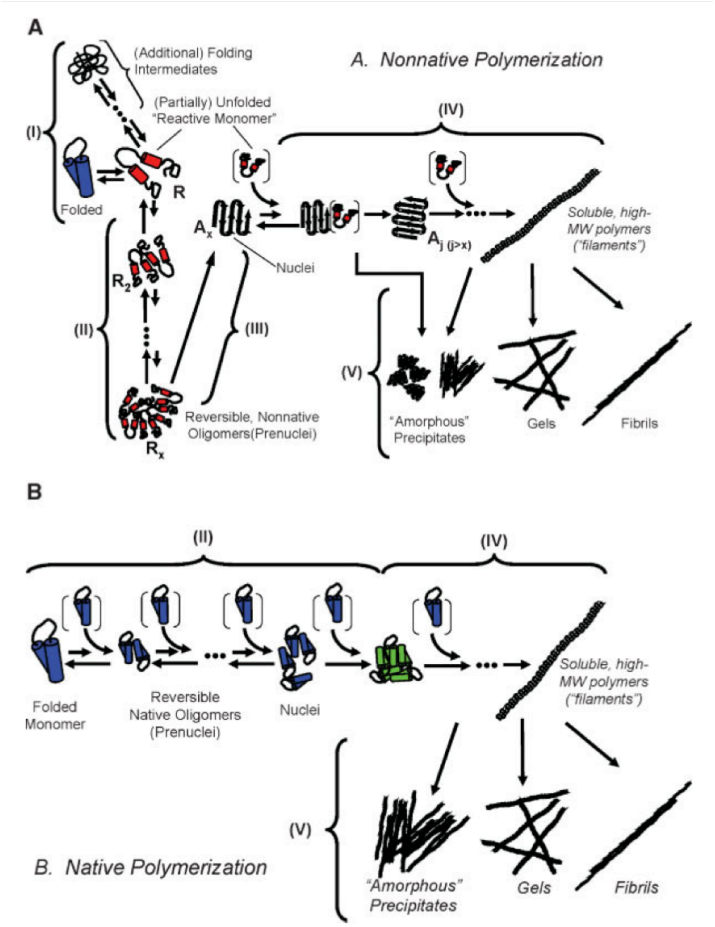

Figure 9.5: Different mechanisms of aggregation of therapeutic proteins (Roberts C.J., Biotechnology and Bioengineering, 98, 5, 2007.)

There are two levels of analysis to achieve this goal. A first simplified description can be captured by monitoring the kinetics of monomer depletion at several protein concentrations

(Figure 9.4, and evaluating an apparent reaction order n, defined as:

$$\frac{dM}{dt} = -k_{\text{app}} M^n, \tag{9.1}$$

Where M is the monomer concentration followed on a few half-lives and k_{app} is the apparent reaction rate constant for monomer loss. The value of n, which typically lye between one and two, reports on the step which is rate limiting in the monomer consumption. In particular, $n = 1$ is indicative that unimolecular conformational changes are rate limiting the kinetics of monomer depletion, whereas $n = 2$ rather corresponds to the case where monomer consumption is rate limited by the aggregation events leading to dimer formation.

A second level of analysis implies a more comprehensive mechanistic description of the full aggregation network. On this purpose, a powerful strategy consists in comparing experimental data with model simulations obtained from a population balance equation scheme that describes the contribution of several individual microscopic reactions. We illustrate this strategy here below, using a case study as a concrete example to guide the explanation. More than the exact content of this very specific example, the student is invited to learn the different steps (here divided in five points) of this general strategy, which can be applied to the analysis of any other system.

9.3.1 Case Study: aggregation of a monoclonal antibody (mAb-1)

1) Experimental Observations

Figure 9.6 shows some experimental observations regarding mAb-1 aggregation. We conclude from these data that, in the case of mAb-1:

(a) The monomer depletion is rate limited by monomolecular conformational changes

(b) Aggregation is irreversible

(c) Aggregates exhibit fractal morphology, with $d_{\text{f}} = 1.85$

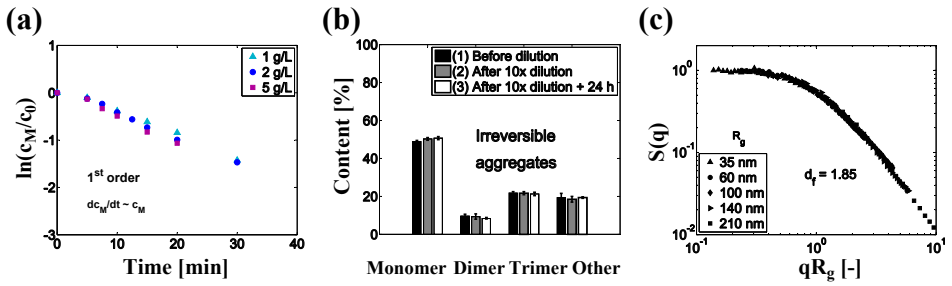

Figure 9.6: Experimental observations for mAb-1. (a) Linearization of the monomer depletion kinetics followed by SEC (b) Dilution experiments to assess aggregates reversibility (c) SLS experiment to measure the fractal dimension of aggregates.

2) Reaction Scheme

According to these observations, the reaction scheme shown in Figure 9.7 is proposed.

(M1-1)	Monomeric conformational changes	$N \overset{k_u}{\rightarrow} U$
(M1-2)	Irreversible oligomer formation	$\begin{cases} U + U \overset{k_{11}}{\rightarrow} U_2 \\ U + U_2 \overset{k_{12}}{\rightarrow} U_3 \end{cases}$
(M1-3)	Irreversible aggregate growth by: monomer addition and cluster-cluster aggregation	$\begin{cases} U + U_i \overset{k_{1i}}{\rightarrow} U_{i+1} & i \geq 3 \\ U_i + U_j \overset{k_{ij}}{\rightarrow} U_{i+j} & i,j \geq 2 \end{cases}$

Figure 9.7: Proposed reaction scheme for mAb-1 aggregation.

First, the monomer in its native form N unfolds to form U, which is a denaturated conformational state of the monomeric protein. This step, denoted as (M1-1) in the kinetic scheme, is regarded as irreversible in this study. Indeed, U can be considered as an intermediate reactive species which is depleted by irreversible aggregation before it can re-fold. Therefore, aggregation is faster with respect to the possible backward reaction of unfolding, and the reversibility of the unfolding step can be neglected. It is worth mentioning that the quantity experimentally accessible from SEC experiments is the sum of the concentrations of N and U, since SEC is not sensitive to changes in protein conformation. The aggregation prone form of the protein, U, can then aggregate to form oligomers, according to step (M1-2). Finally, aggregates grow irreversibly either by monomer addition or by cluster-cluster aggregation, as depicted in step (M1-3).

The unfolding step is a simple monomolecular reaction, which can be easily described by a single kinetic rate constant k_U. Describing the aggregation steps is a bit more challenging, though, as it requires the definition of an aggregation kernel which provides a relation between aggregate size and aggregate reactivity. Following the approach presented before in the case of polymer colloids, we first

compute the characteristic time for rapid coagulation so as to determine whether or not aggregation occurs under diffusion limited conditions. At 70 °C, with a protein concentration of 1 g/L, we obtain $t_{\mathrm{RC}} \approx 10^{-5} s$. Therefore, we conclude that aggregation is not limited by diffusion under these conditions, and we select the traditional RLCA kernel to describe aggregate growth.

However, it must be emphasized that this kernel was derived in the case of spheres uniformly charged, while it is known that protein reactivity strongly depends on protein conformation and on the accessibility of aggregation-prone patches. This effect can be accounted for by introducing different values of the Fuchs stability ratio in order to characterize the stability of different sub-populations of species characterized by a similar reactivity. In particular, the unfolded aggregation-prone monomer U is an unstable intermediate which has a very high reactivity compared to other aggregates species. Therefore, three types of aggregation events characterized by species with different reactivity can be identified: monomer-monomer, monomer-aggregate and aggregate-aggregate. Accordingly, three Fuchs stability ratios are defined: W_{11},$W_{1\mathrm{j}}$ and W_{ij}, which describe oligomer formation, aggregate growth by monomer addition and aggregate growth by cluster-cluster aggregation, respectively.

3) Population Balance Equations

The kinetic model corresponding to the reaction scheme of Figure 9.7 is given below:

$$\begin{cases} \dfrac{\mathrm{d}N}{\mathrm{d}t} = -k_U N \\ \dfrac{\mathrm{d}U}{\mathrm{d}t} = k_U N - U \sum\limits_{j=1}^{\infty} k_{1,j} U_j \\ \dfrac{\mathrm{d}U_{i\geq 2}}{\mathrm{d}t} = \frac{1}{2} \sum\limits_{j=1}^{i-1} k_{j,i-j} U_j U_{i-j} - U_i \sum\limits_{j=1}^{\infty} k_{i,j} U_j \end{cases} \tag{9.2}$$

With:

$$\begin{cases} k_{i,j} = k_s B_{i,j} P_{i,j} W_{i,j}^{-1} \\ k_s = 8 k_B T / 3\eta \\ B_{i,j} = \frac{1}{4} \left(i^{-1/d_{\mathrm{f}}} + j^{-1/d_{\mathrm{f}}} \right) \left(i^{1/d_{\mathrm{f}}} + j^{1/d_{\mathrm{f}}} \right) \\ P_{i,j} = (ij)^{\lambda} \end{cases} \tag{9.3}$$

And $W_{11} \neq W_{1\mathrm{j}} \neq W_{\mathrm{ij}}$

It can be observed that the usual Smoluchowski population balance equations were modified in order to account for two features that are specific of proteins: (1) an unfolding step was introduced to reflect monomolecular changes in protein conformation, (2) several Fuchs ratio values were introduced to describe the different reactivities of the various sub-populations present in solution.

4) Parameter Estimation

The implementation of the proposed kinetic scheme requires the estimation of several parameters. Some of these parameters can be evaluated by independent measurements, while others can be estimated by fitting the suitable quantities to those measured experimentally as a function of time. Since the concentration of U is low and nearly constant due to its high reactivity, the unfolding rate constant k_{U} can be approximated to k_{app}, which is determined from the linearization of the experimental monomer depletion. The fractal dimension has been measured by SLS and the power law factor λ appearing in the aggregation kernel has been estimated as $\lambda \approx 1 - 1/d_{\mathrm{f}}$. The remaining parameters are the three Fuchs ratios which have been fitted to describe the experimental data at the reference protein concentration of 2 g/L. The parameters used for the simulations are summarized in Table 9.1.

Parameter	k_U	d_f	λ	W_{11}	W_{1j}	W_{ij}
Value	$1 \times 10^{-3} s^{-1}$	1.85	0.5	8.5×10^6	4×10^7	8×10^8
Source	k_{app}	SLS Exp.	$1 - 1/d_f$	Fit	Fit	Fit

Table 9.1: Parameters used for the simulations of mAb-1 aggregation (without co-solutes).

In Figure 9.8 (a-c) it can be seen that the simulations are in excellent agreement with the experiments, indicating that the proposed kinetic model can successfully describe the aggregation of mAb-1 under the investigated conditions.

The comparison between the different Fuchs stability ratios estimated by the fitting to experimental data provides information on the relative reactivity of the various species involved in the aggregation process.Considering the values reported in Table 9.1, it can be noticed that$W_{1\mathrm{j}} \ll W_{\mathrm{ij}}$. This highlights that, for this system, aggregate growth by monomer addition prevails over aggregate growth by cluster-cluster aggregation, probably due to the high reactivity of the unfolded monomer.

5) Model Validation

To further validate the proposed kinetic scheme, the kinetics of aggregation were simulated at protein concentrations of 1 g/L and 5 g/L using the same set of values reported in Table I, with no additional parameters. In Figure 9.8 (d-i), it can be seen that the model predictions agree very well with all the experimental results, proving that the model is capable of predicting the concentration effect on the aggregation kinetics of mAb-1 in the concentration range

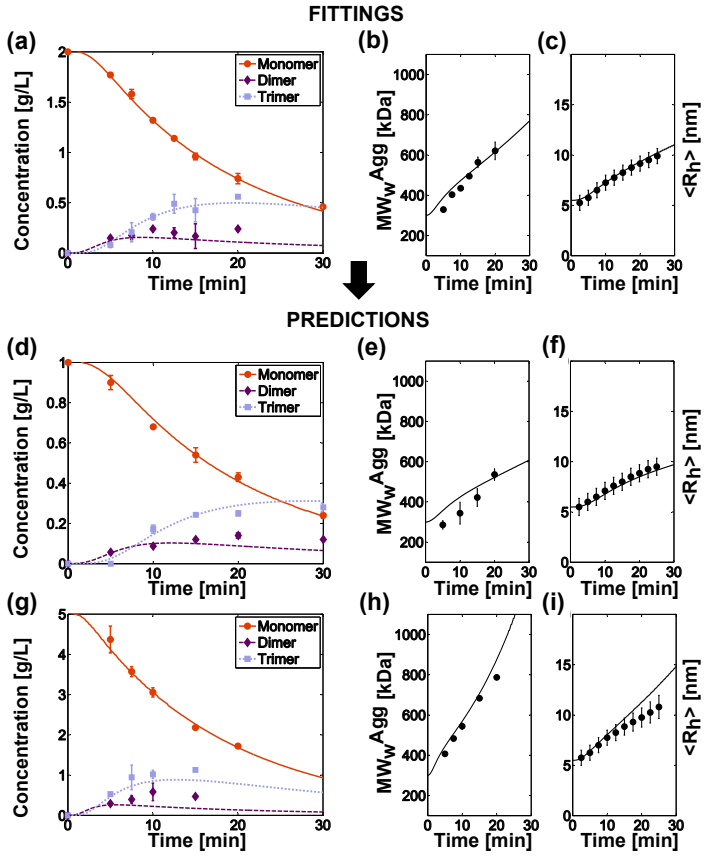

Figure 9.8: Comparison between experimental data and simulations for mAb-1 at protein concentration of 2 g/L (a-c), 1 g/L (d-f) and 5 g/L (g-i). The experimental concentration of monomer, dimer and trimer were determined by SEC. The aggregate molecular weight was measured by SEC-MALS and the average hydrodynamic radius was followed by DLS.

from 1 g/L to 5 g/L. We can therefore conclude that the kinetic scheme of mAb-1 aggregation is the one presented in Figure 9.9.

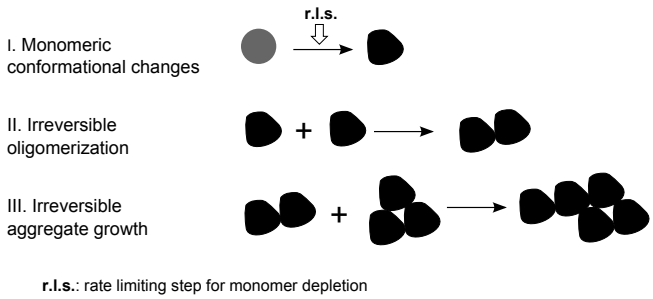

Figure 9.9: Kinetic scheme for mAb-1 aggregation

9.4 Protein Misfolding and Aggregation in the Biomedical Context

9.4.1 Functional role of protein self-assembly and aggregation in biology

Several proteins play theri biological roles in a self-assembled state. For instance, under physiological conditions insulin is present as an hexamer which is coordinated by a zinc ion. Another relevant example is represented by molecular chaperones. These proteins are crucial components of the protein homeostasis network, and assist proteins in folding correctly as well as in the removal of degraded species. Relevant chaperones are heat shock proteins, which are over-expressed as an answer to a rise in the temperature, clusterin, alpha-B crystallin. The vast majority of molecular chaperones are present as a distribution of oligomers in dynamic equilibrium. Different oligomers have different reactivity, and this quaternary structure is crucial to allow molecular chaperones to react to different situations and interact with different protein structures.

In other cases, biology uses larger forms of protein aggregates. A particular type of protein aggregate structure which has been increasingly found in nature is represented by amyloid fibrils. These aggregates exhibit a regular fibrilar geometry, with a diameter of 5-10 nm and a length of 1-10 μm. Peptide and protein hormones in secretory granules of the endocrine system are stored in an amyloid-like cross-beta-sheet-rich conformation (Maji, S.K. et al., Science. 2009; 325(5938):328-32). Thus, functional amyloids in the pituitary and other organs can contribute to normal cell and tissue physiology. This colloidal state guarantees a controlled release of functional monomeric hormones in response to a change of the environment, for instance the pH. Functional amyloids are also fungal prions, which are involved in prion replication, and the amyloid protein Pmel17, which is involved in mammalian skin pigmentation. Functional amyloids have also been observed in many bacteria, where they are associated to host cell adhesion and invasion, and they are potent inducers of the host inflammatory response (Barnhart and Chapman, Annual Review of Microbiology, 60, 131-147, 2006).

9.4.2 Role of aberrant protein aggregation in pathology: amyloid fibrils

(Reference: Knowles, T.P.J. et al., The amyloid state and its association with protein misfolding diseases. Nat. Rev. Mol. Cell Biol., 2014, 15 (6), 384-396) Although amyloid fibrils are increasingly associated to biological functions, they were intially discovered in the context of pathological states. In particular, these peculiar protein aggregates are associated with the onset and development of a large number of neurodegenerative diseaeses, including Alzheimer's and Parkinson's disorders, Amyotrophic Lateral Sclerosis and systemic amyloidosis.

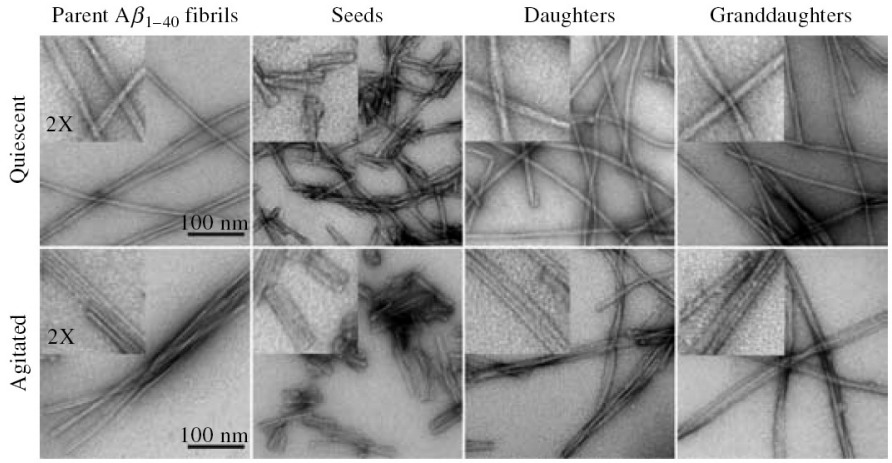

Figure 9.10: TEM images of amyloid fibrils

The medical doctor Aloises Alzheimer was the first scientist who associated these structures observed in the brain of people affected by the disease wit the loss of neuron function. Initially, these structures were thought to consist of starch (from which the word amyloid). However, later it was discovered that they were made of proteins.

In many cases, the formation of amyloid fibrils follows the incorrect folding of the protein, a process defined as misfolding. If the protein can not form the correct intramolecular bonds require to fold correclty, it can interact with other molecules to form aggregates. A very important observation is that a large variety of proteins can form amyloid fibrils under suitable conditions. Moreover, even if the monomeric proteins have very few or no properties in common, the amyloid fibrils share a large number of features, including in particular the

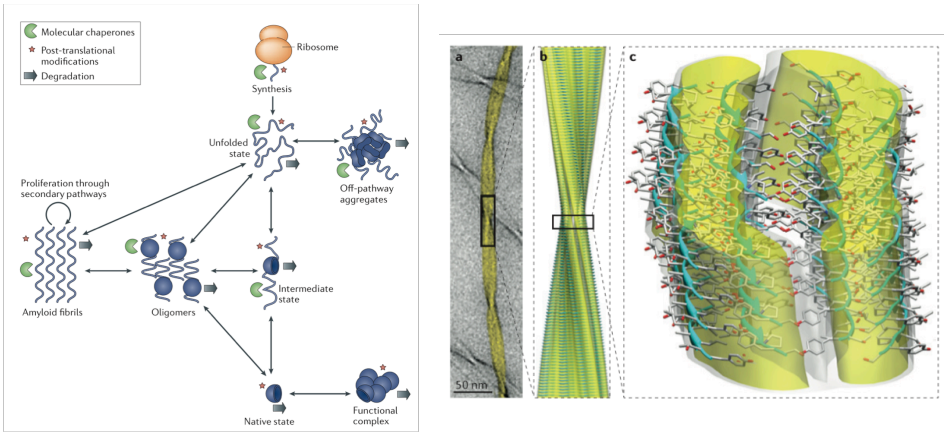

Figure 9.11: Protein Misfolding and Amyloid Fibrils

morphology and a high content of secondary beta sheet structures. These observations induce people to consider amyloid fibirls as an alternative form of folding, and some hypothesis consider the simple amyloid structure as the primordial form of folding, which has evolved during the years into more complex 3-D structures.

An increasing series of evidence, including mutational studies, associate amyloids witht the onset and development of the disorders. However, the connection between the aggregation process and the lost of function is still largely unclear. Small reactive intermediates, which are formed during the aggregation pathway leading to the formation of fibrils, are currently thought to represent the most toxic species. These intermediates, broadly defined as oligomers, could damage neuronal cells via a series of processes, including membrane perforation, activation of a cascade of signal and sequestration of key functional proteins.

The problem is clearly very complex and interdisciplinary, involving contributions from clinical doctors, biologists, biochemists and biophysicists. Since amyloid fibrils are colloids, several aspects of this stability problem share physico-chemical features with the systems discussed in this course, as .described in the following paragraphs.

9.4.3 Kinetic and thermodynamic stability of amyloid fibrils

The main driving force for the formation of amyloid fibrils is their high thermodynamic stability. The beta sheet structures allow the formation of a large number of intermolecular hydrogen bonds, which are energetically very favorable. This explains why so many different proteins

can convert into the amyloid state.

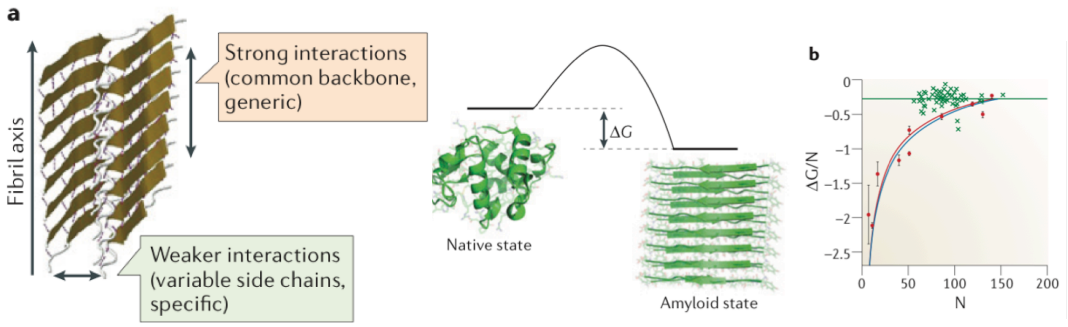

Figure 9.12: Thermodynamic stability of amyloid fibrils

Since the aggregation process is concentration dependent, there is a critical concentration (dependent on the thermodynamics of the process) determining the stability or instability of a protein solution. For many proteins under physiological conditions this critical concentration is close to the physiological value: this observation indicates that proteins in biological systems could be thermodyanamic unstable and only kinetically stable

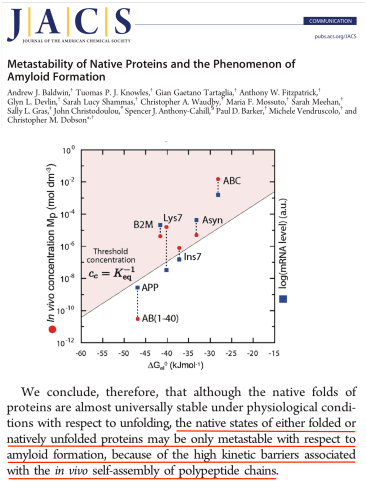

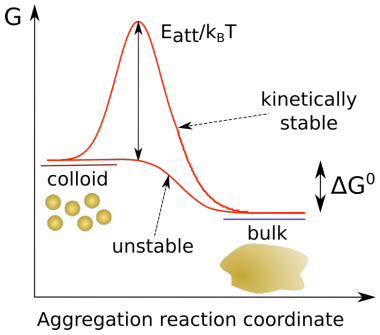

Energy barrier:
Intermolecular forces
stability time ∝ E/k_BT

Figure 9.13: Kinetic stability of amyloid fibrils

9.4.4 Aggregation mechanism of amyloid fibrils

The kinetics of the aggregation process plays therefore an important role in amyloids. In analogy with Chapter 7, we can decribe the time evolution of the fibril size distribution by applying a population balance equation, replacing the concentration of particles N_i with the concentration of fibrils containing j monomeric units, f_j.

There are, however, some differences in the aggregation mechanism that must be captured in the PBE (Figure 9.14): since aggregation occurs only in one dimesion at the fibril ends, the aggregation step is replaced by elongation, with a rate constant k_+ which is independent on the fibril size (in contrast with the aggregation kernels described in Chapter 7) and only f_{j-1} and f_j partecipate in the mass balance of f_j. Additionally, we have to consider primary nucleation and secondary nucleation events, which appear in the mass balances of the smallest fibrils (containing n_C and n_2 monomeric units). Typical secondary nucleation reactions are: a) surface-induced secondary nucleation, where the surface of the existing fibrils promotes the formation of new fibril. The rate is therefore proportional to the total mass (surface) of the fibrils in the system; b) fragmentation, because a breakage event creates two new fibril reactive ends. In the descriptio of fragmentation (breakage), we have again the problem of the daughter distribution. We can assume the same probability of breakage for each bond within a fibril, which implies that a fibril with j monomeric units has $j-1$ positions where brekage can occur. We note that the fibrillar morphology of amyloids can be considered an extreme case of the fractal aggregates discussed in Chapter 7 with $d_f = 1$. The PBE can be expressed as:

$$\frac{\mathrm{d}f_j}{\mathrm{d}t} = 2k_+ f_{j-1} - 2k_+ f_j - k_-(j-1)f_j + 2k_- \sum_{i=j+1}^{\infty} f_i + \delta_{j,n_C} k_n m^{n_C} + \delta_{j,n_2} k_2 M m^{n_2} \tag{9.4}$$

where $m(t)$ is the monomer concentration, $M = \sum_{i=n_C}^{\infty} i f_i$ is the total fibril mass concentration and the Kronecker delta operators δ_{j,n_C} and δ_{j,n_2} are equal to one for $j = n_C$ or $j = n_C$, and zero otherwise. The first term on the right side of the equation accounts for the generation of filaments of length j by monomer addition to a shorter fibril; the second term describes the disappearance of the fibrils of length j which grow further to length $j+1$; the third and fourth terms are related to fragmentation events and the last terms refer to the generation of new nuclei by primary and secondary nucleation events with reaction orders n_C and n_2, respectively. Recently available analytical solutions of the master equation led to closed expressions of the time evolution of the principal moments of the fibril distribution, i.e., the fibril number

concentration, $M = \sum_{i=n_C}^{\infty} f_i$ and the fibril mass concentration, $M = \sum_{i=n_C}^{\infty} i f_i$, and provided insights into the relationship between relevant physical quantities of the system.

An important application of the PBE is the possibility to extract information about the relative contribution of different microscopic events on the total fibril mass formation (the macroscopic experimental observable). This operation is relevant in many contexts, including the discovery of molecules which could block the aggregation process in vivo, as discussed in the next paragraph.

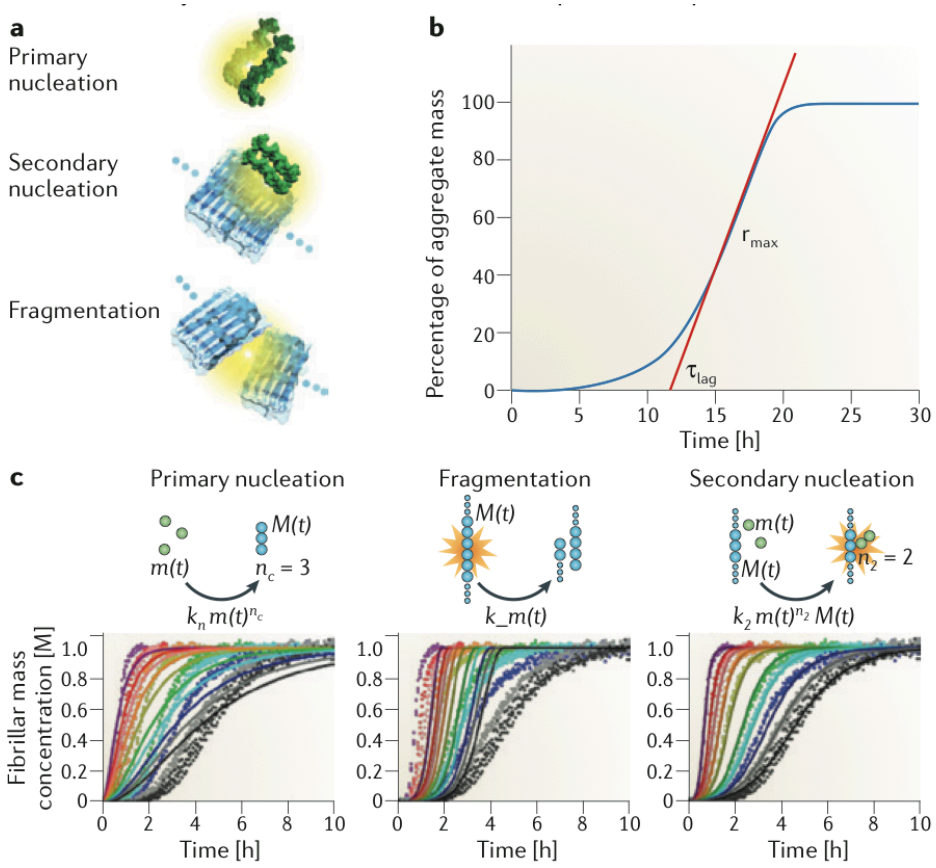

Figure 9.14: Microscopic aggregation mechanism of amyloid fibrils

9.4.5 Role of chemical kinetics in drug discovery

Information about the microscopic processes underlying changes in macroscopic variables are crucial for understanding the mechanism of action of a given drug as well as for identifying strategies to change both the thermodynamics and the kinetics of the disease-associated

processes. This general strategy has found widespread applications in enzymology, where chemical kinetics has become a standard tool for testing inhibition mechanisms, including identifying competitive, uncompetitive and non-competitive inhibition mechanisms (Chapter 8). This approach has already resulted in significant progress in the understanding of the mechanisms of action of enzymes and has led to the development of anti-cancer drugs targeting kinases activity.

The exact causative relationship between amyloid formation and organ dysfunction remains unclear, but the inhibition of protein aggregation is an attractive candidate for generating disease modifying therapeutic strategies against Alzheimer's disease and other neurodegenerative disorders because in all cases the toxicity has been associated to the soluble forms of the aggregating peptides. In this context, kinetics is not only a tool to investigate the inhibition mechanism but can represent also a therapeutic target per se, since the delay of the aggregation process for a sufficiently large number of years can be considered as effective as the thermodynamic inhibition of the process. However, either a thermodynamic or a kinetic inhibition should not aim at a generic arrest or delay of the formation of the final fibril load, but rather at a specific intervention on the molecular species that mediate cellular toxicity. Indeed, an uncontrolled disassembly of higher order aggregates, thought to be relatively inert in a biological context, could lead to the increase in the concentration of soluble toxic oligomers and hence negative outcome in terms of rescuing toxicity. In order to develop effective therapeutic strategies, therefore, an understanding is required not only of the protein aggregation process and its connection to pathogenicity, but also of how potential drugs interfere with these processes.

We can apply the population balance equation platform to understand the inhibition mechanism of fibril formation at the molecular level. The key for applying this approach to analyse inhibition of aggregation is to note that the change in different microscopic events results in different characteristic macroscopic aggregation profiles, as shown qualitatively in the model simulations in Figure 9.15. For instance, the decrease of primary nucleation rate increases the lag-time preceding the growth phase. Elongation and secondary nucleation events have different effects on both lag-phase and growth, Surface induced secondary nucleation events become relevant at larger conversion values. As a consequence, a reduction of this microscopic step does not affect significantly the aggregation profile at low conversion values. By contrast, a decrease of the elongation rate constant inhibits the formation of fibrils from the early stages of the process. and therefore we can discriminate the inhibition of these two microscopic processes by considering the macroscopic profile of the kinetics of aggregation at different protein and inhibitor concentrations.

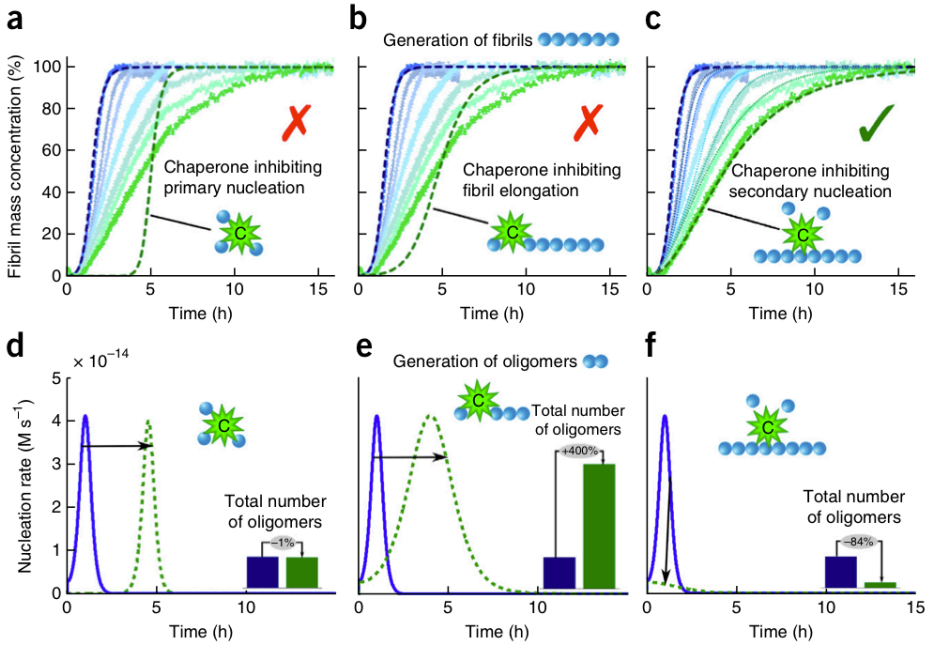

Figure 9.15: Kinetic modelling analysis of aggregation inhibition mechanism. The binding between the inhibitor (for instance, a molecular chaperone) and the different species in the system leads to specific changes in the microscopic steps of the aggregation process, such as primary nucleation, elongation and secondary heterogeneous processes. (a-c) Dot lines represent model simulations of the macroscopic time evolution of fibril formation, showing how changes in single specific microscopic aggregation events affect in a characteristic way the observed kinetic macroscopic profile (simulations are compared to experimental data, reported in different colors). (d-f) Different modalities of intervention have dramatically different consequences on the concentraiton of toxic oligomers generated during the aggregation process.

It is important to observe that the specific inhibition of heterogeneous processes delays the fibril formation but does not affect the final fibril load, since monomers are still consumed by elongation events. To affect the final fibril composition, a thermodynamic inhibition which prevents primary nucleation and elongation processes is required. On the other hand, the kinetic inhibition of secondary processes can suppress the generation of toxic intermediates, in contrast to the kinetic inhibition of primary nucleation and elongation processes, which delays but not suppresses the formation of soluble oligomers. For the specific system under consideration, calculations based on the kinetic model can quantify the qualitative aspects describe above, leading to the identification of the inhibition strategy with the best potential therapeutic benefits.